

Histologic and histomorphometric results of three bone graft substitutes after sinus augmentation in humans

Marzia Pettinicchio · Tonino Traini ·
Giovanna Murmura · Sergio Caputi · Marco Degidi ·
Carlo Mangano · Adriano Piattelli

Received: 14 June 2010 / Accepted: 18 October 2010 / Published online: 3 November 2010
© Springer-Verlag 2010

Abstract The aim of this study was to compare the histological behavior of three bone graft materials placed in human. The comparison was made among Bio-Oss® (BO), Engipore® (EP), and PepGen P-15® (P-15). Five biopsies for each group of biomaterial, retrieved 6 months after sinus lift augmentation, were analyzed. The investigation was carried out using light microscope (LM), scanning electron microscope (SEM) with an energy dispersive spectrometer (EDS), and circularly polarized light microscope (CPLM). Under LM, the amount of newly formed bone was significantly higher in BO than P-15 ($P < .05$), while the amount of residual graft material was significantly higher in P-15 than BO ($P < .05$). The extension of marrow spaces was significantly higher in EP than both BO and P-15 ($P < .05$). SEM-EDS analysis showed a Ca/P ratio of 1.8 for BO, 2.2 for EP, and 1.5 for P-15. Under CPLM, BO showed no significant difference for transverse ($18.4 \pm 2.7\%$) and longitudinal ($16.3 \pm 1.8\%$) bone collagen fibers ($P = .195$); EP showed a significant difference between transverse ($4 \pm 0.7\%$) and longitudinal ($7.6 \pm 2.5\%$) bone collagen fibers ($P = .015$);

finally, P-15 showed no significant difference for transverse ($3.8 \pm 1.6\%$) and longitudinal ($4.9 \pm 1.2\%$) bone collagen fibers ($P = .279$). No investigated biomaterial was completely resorbed, but all the residual particles demonstrated a close bone integration to form a hybrid tissue. BO particles appeared perfectly osseointegrated in the trabecular bone. EP showed a tendency to concentrate the bone apposition into the microporosities; P-15 particles appeared bridged by newly formed bone trabeculae.

Keywords Bone grafted material · Bone regeneration · Bovine bone · Electron microscopy · Sinus augmentation

Introduction

Rehabilitation of the edentulous patients with dental implants may be a problem because of insufficient bone volume as a result of alveolar atrophy and pneumatization of the maxillary sinus. In this anatomical situation, it can be very difficult to obtain an effective primary stability due to the absence of a useful quantity of cortical bone and for the loose structure of type IV trabecular bone [1]. The maxillary sinus augmentation procedure, firstly presented by Tatum in 1976, has proved to be an effective treatment option [2, 3]. Various grafting materials have been used for sinus augmentation: autologous bone, mineralized and demineralized freeze-dried allograft, coralline calcium carbonate, bioactive glass, polylactide-polyglycolide materials, synthetic polymers, calcium sulfate, anorganic bovine bone, and hydroxyapatite (HA) [4–10]. Autologous grafts are considered the golden standard in terms of osteogenic potential, but they are of limited availability, and the necessity of harvesting bone chips from another skeletal site requires an additional surgical procedure with the associated

M. Pettinicchio · T. Traini (✉) · G. Murmura · S. Caputi ·
A. Piattelli
Department of Oral Sciences, Nano and Biotechnologies,
University of Chieti-Pescara,
Via dei Vestini, 31,
66100 Chieti, Italy
e-mail: t.traini@unich.it

M. Degidi
Private Practice,
Bologna, Italy

C. Mangano
Private Practice,
Gravedona (COMO), Italy

risk of morbidity at the donor site [11, 12]. Yet, a resorption of autologous bone grafts (up to 56% of cortical bone grafts in 4 months) was reported in both animal and human studies [13–15]. Synthetic materials are therefore an attractive alternative since they are potentially available in unlimited amounts, in a range of different sizes and shapes, and can be modified in order to act as matrix carriers for the delivery of drugs, hormones, growth factors, and stem cells. BO (Bio-Oss®, Geistlich Pharma, Wolhusen, Switzerland) has shown excellent osteoconductive properties and promising results in sinus floor elevation procedures [16]; moreover, it promotes osteogenesis and shows very low resorbability [17, 18]. BO is a sterilized bovine bone delivered in granules of 10 µm, almost completely deproteinized with 75% to 80% of porosity. It is mainly formed by natural HA, as the bone tissue is. The HA in the mineralized phase of bone has a fraction of calcium (Ca) of 39.9% and phosphorus (P) of 18.5%, with a Ca/P ratio of 1.667 at/at.% (2.15 wt/wt.%) [19]. In normal calcified bone, the Ca/P molar ratio increases with increasing calcification [20]. EP (Finceramica srl, Faenza, Italy) is a porous HA ceramic with osseointegrative properties able to generate bone formation in non-bony intramuscular sites [21–24]. Because of high affinity for bone morphogenetic proteins (BMPs), porous HA was used as a carrier for locally produced and released BMPs/osteoprogenitors, capable of inducing osteoblasts differentiation and new bone formation [25–27]. BMP family members, in fact, were recovered within the concavities of the porous HA at the interface with generated mesenchymal tissue [28]. It was reported [29, 30] that new bone formation starts in concavities rather than on plane or convex surfaces, and the shape of the concavities can affect cellular morphology. Moreover, the ability of the material to support angiogenesis and growth of vasculature has been cited as a key factor in bone formation [31] and finally bone regeneration, as confirmed by several *in vitro* and *in vivo* experimental studies in animals [26–29] and humans [21, 31–33]. EP is a porous engineered pure HA with about 90% porosity. The HA crystal structure is very similar to that of bone [34]. P-15 (DENTSPLY-Friadent, Ceramed, Lakewood, CO, USA) is a natural anorganic bovine-derived HA matrix coupled with a synthetic cell-binding peptide (P-15; 200 ng of P-15 with 1 g of HA matrix) [35, 36]. The particle size range of 250–420 µm has a mean pore volume of 0.13 cm³/g and a total porosity of 28% [37]. P-15 peptide is absorbed on HA matrix in a saturable manner [38]. P-15 has been shown to stimulate the role of native collagen matrix in wound repair, producing an enhanced cell adhesion and matrix remodeling [39], while the calcium phosphate needed for osteoconduction is provided by the HA matrix [40]. Good clinical results have been obtained in bone regeneration procedures [37, 41, 42]. P-15 accelerates the early bone formation and stimulates osteoblasts to express TGF-beta-1 [43] and increases actin

stress fibers in cells attached on a bone substitute surface, suggesting an enhanced cell adhesion [44]. The aim of the present study was to identify and compare histological behavior of these three different bone-substitute graft materials placed in humans after sinus augmentation, evaluating the microstructure of the new composite tissue formed (bone plus biomaterial), the Ca/P ratio of the materials, that may add to our understanding of the changes occurring at the bone–biomaterial interface, and finally to obtain information about the amount of regenerated bone and the collagen fiber orientation in newly formed bone, marrow spaces, and residual particles. It must be stated that sinus augmentation was considered as a standardized procedure suited to compare biomaterials.

Patients and methods

Ethical considerations

This study is consistent with the ethical principles enunciated from the Declaration of Helsinki. All the specimens evaluated in the present retrospective study were obtained from clinical practice. During the implant placement, as we usually do in dental practice, a 2.5-mm trephine bur was used instead of the pilot bur in order to collect bone tissue to be employed in case bone autograft is needed. The unused bone cores, generally thrown, after informed written consent obtained from each patient, were used in the present study.

Surgical and clinical procedure

All the patients were treated by the same surgeon in the private practice in Gravedona (CM) and Bologna (MD). The patients were draped to guarantee maximum asepsis. The skin was disinfected with betadine, and the patient was asked to rinse with clorexidine mouthwash 0.2%. Under local anesthesia, a crestal incision, slightly toward the palatal aspect throughout the entire length of the edentulous segment, was performed supplemented by buccal releasing incisions mesially and distally. Full thickness flaps were elevated to expose the alveolar crest and the lateral wall of the maxillary sinus. Using a round bur under cold (4–5°C) sterile saline irrigation, a trap door was made in the lateral sinus wall. The door was rotated inward and upward with a top hinge to a horizontal position. The sinus membrane was elevated with curettes of different shapes, until it became completely detached from the lateral and inferior walls of the sinus. All the biomaterials were mixed with venous blood and carefully packed in the sinus cavity, especially in the posterior and in the anterior part. BO particles were approximately 10 µm in diameter; the pore distribution of

EP was homogeneously bimodal with approximately 32% pores between 100 and 200 μm diameter and approximately 40% pores 200–500 μm diameter; finally, the particle size of P-15 was between 250 and 420 μm in diameter. Flaps were sutured. Antibiotics and analgesics were given for 1 week. Sutures were removed 2 weeks after surgery. In the postoperative period, the patients were followed up at monthly intervals until implant placement that was carried out for all groups after a mean (\pm SD) healing period of 6 (\pm 0.5) months. At the time of the implant surgery, a 2.5-mm trephine bur (Straumann, Waldenburg, Switzerland) was used instead of the first bur for implant bed preparation in order to retrieve a bone core to be used in case of necessity near the implant collar. On total of 15 retrieved specimens, only 13 were used since two bone cores were used to improve the implant bed site. No membrane was used. Complete wound closure was performed with non-resorbable sutures.

Histologic specimen processing

The human specimens were fixed in 10% buffered formalin, dehydrated in an ascending series of alcohol, rinsed and embedded in a glycolmethacrylate resin (Techonovit 7200 VLC, Kulzer, Wehrheim, Germany). After polymerization, the specimens were sectioned, along their longitudinal axis, with a high-precision diamond disc at about 150 μm , and ground down to about 30 μm with a custom built sawing and grinding apparatus (TT System, TMA2, Grottammare, Italy).

Transmitted light microscopy (LM)

The histomorphometry was used to evaluate both the quality and the quantity of bone around the particles of the biomaterials. The slides were stained with acid fuchsin and toluidine blue. The investigation was carried out in a transmitted brightfield light microscope (Laborlux S, Leitz, Wetzlar, Germany) connected to a high resolution video camera (3CCD, JVC KY-F55B, JVC®, Yokohama, Japan) interfaced to a monitor and PC (Intel Pentium III 1200 MMX, Intel®, Santa Clara, CA, USA). This optical system was associated with a digitizing pad (Matrix Vision GmbH, Oppenweiler, Germany) and a Histometric software package with image capturing capabilities (Image-Pro Plus 6.0, Media Cybernetics Inc., Immagini & Computer Snc, Milano, Italy).

Circularly polarized light microscopy (CPLM)

Birefringence was used to evaluate the bone microstructure around particles of biomaterials using polarized light. Unstained sections of 100 μm in thickness were used.

Collagen fibers orientation was evaluated by observing the sections under a light microscope (Axiolab, Carl Zeiss, Jena, Germany) equipped with two linear polarizer and two quarter wave plates arranged to have transmitted circularly polarized light. Collagen fibers aligned perfectly transverse to the direction of the light propagation (parallel to the plane of the section) appeared “white-blue” due to a change in the refraction of exiting light, whereas the collagen fibers aligned along the axis of light propagation (perpendicular to the plane of the section) appeared “red-yellow” because no refraction occurred.

Scanning electron microscopy (SEM)

To investigate the relationship between biomaterial particles and bone, the specimens were polished with 0.5 μm alumina to an optical finish, were light etched with 0.1 N of HCl solution for 10 s, were treated with trypsin (80 U/ml) at pH of 7.4 for 15 min at 37°C, and were lightly sputter-coated with gold (Emitech K 550, Emitech Ltd, Ashford, Kent, UK). The specimens were placed on the storage of a scanning electron microscope (SEM) with LaB6 (Zeiss EVO 50 XVP, Carl Zeiss SMY Ltd., Cambridge, UK), equipped with tetra solid-state BSE detector. SEM operating conditions included 30 kV accelerating voltage, 15 mm working distance, and 1.2 nA probe current. The images were captured with 20 scans using a line average technique. To perform a compositional analysis for calcium and phosphorus concentration, an energy dispersive spectrometer (EDS; INCA, Oxford Instruments, Oxon, UK) was used.

Statistical analysis

Statistical analysis was performed by means of the computerized statistical package (Sigma Stat 3.5, SPSS Inc., Ekrath, Germany). The differences among the means of histomorphometric results were made using either Kruskal-Wallis or ANOVA test, depending on data distribution, while the evaluation of multiple comparison procedures was made always using Tukey test; the variation of the amount of transverse and longitudinal collagen fibers orientation inside each group was made using unpaired *t* test. A *P* value of under 0.05 was considered statistically significant.

Results

Patient description

Based on a parallel group design, five patients were treated with BO (three female, two male; mean age of 51.6 \pm

4.3 years), five patients with Engipore (five female; mean age of 52.4 ± 1.2 years), and five patients with P-15 (two female, three male; mean age of 54.4 ± 2 years). No patient was a smoker, with osteoporosis, or with diabetes or irradiation. All the treated patients were in good health condition and with presence of 1.5–3 mm of crestal bone between the sinus floor and the alveolar ridge.

Newly formed bone

Light microscopy showed that the BO particles were surrounded by woven bone with some area of mature bone with well-organized osteons. In some fields, osteoblasts were observed in the process of apposing bone directly on the particle surface. No gaps were present at the bone–particles interface, and the bone was always in close contact with the particles. Most of the particles were joined by the

newly formed bone (Fig. 1, A). At higher magnification, the bone presented wide osteocytic lacunae (Fig. 1, A1). In EP specimens, the newly formed bone was in close contact with the biomaterial's particles. No gaps were present at the bone–biomaterial interface (Fig. 1, B). In some areas, at the interface, there were osteocytes in contact with the biomaterial surface (Fig. 1, B1). Finally, in P-15 specimens, the newly formed bone was in close contact with the particles, surrounding and bridging most of them (Fig. 1, C). No gaps, connective, or fibrous tissues were found at the bone–biomaterial interface (Fig. 1, C1). Osteoid matrix, lightly stained by acid fuchsin, was present in some portions of the interface. The newly formed bone mean rate (\pm SD) was $38 \pm 2.1\%$ for BO, $38.5 \pm 4.5\%$ for EP, and finally, $28.2 \pm 1\%$ for P-15. Statistical analysis showed that there was a significant difference only between BO and P-15 ($P < .05$; Fig. 1, D).

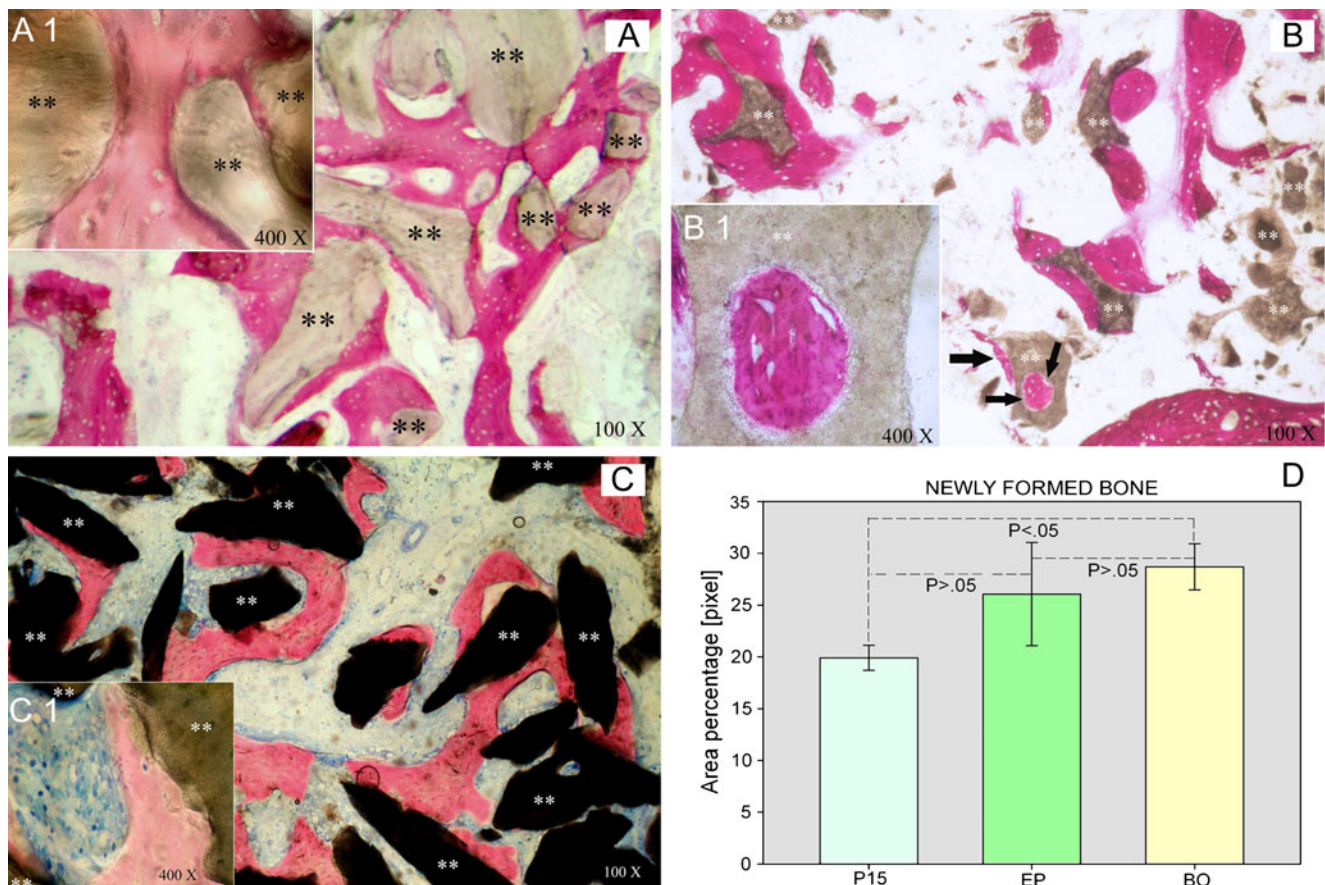


Fig. 1 *A* At $\times 100$ magnification, the BO particles (double asterisks) appeared to be covered and joined by newly formed bone (in red). Acid fuchsin-toluidine blue staining. *A1* At $\times 400$ magnification, an intimate contact between bone and grafted particles (double asterisks) was present. *B* At $\times 100$ magnification, the EP particles (double asterisks) were covered by newly formed bone (in red). Acid fuchsin-toluidine blue staining. *B1* At $\times 400$ magnification, the small pores

appeared completely filled by newly formed bone. *C* At $\times 100$ magnification, the P-15 particles (double asterisks) appeared bridged by newly formed bone (in red). Acid fuchsin-toluidine blue staining. *C1* At $\times 400$ magnification, newly formed bone (in red) appeared to grow inside the biomaterial particles. *D* Area percentage of newly formed bone vs. type of biomaterial. Kruskal–Wallis and Tukey tests

Residual particles

No inflammatory cell infiltrate was present around the particles of the different biomaterials or at the interface with bone (Fig. 1, A, B, C). Marked staining differences were present from the host bone and biomaterial particles since they had a lower affinity for the dyes. Only in a very few areas of BO specimens, it was possible to see multinucleated giant cells. For EP, in the regions where bone was not in contact with the biomaterial particles, some areas of resorption were visible on the particle surfaces itself. P-15 showed in some regions interdigitations of newly formed bone that entered and connected the surface of the biomaterial particles; the bone tissue apparently had grown inside the material. The residual graft material mean rate (\pm SD) was $29\pm 1.8\%$ for BO, $12\pm 2.3\%$ for EP, and finally, $36.7\pm 1.6\%$ for P-15. Statistical analysis showed that there was a significant difference between BO and EP, and EP and P-15 ($P < .05$; Fig. 2).

Marrow spaces

Marrow spaces together with newly formed bone could be considered a density index of the regenerated tissue, which played an important role during the implant placement for the primary stability of the implants. The marrow spaces mean rate (\pm SD) was $36\pm 1.3\%$ for BO, $44.6\pm 4.2\%$ for EP, and finally, $33.9\pm 1.1\%$ for P-15. Statistical analysis showed that there were significant differences among EP and both BO and P-15 ($P < .05$; Fig. 3).

Bone collagen fiber orientation

Under circularly polarized light microscopy (CPLM), the bone around the BO appeared characterized by well-oriented collagen fibers (Fig. 4, A). Transverse collagen

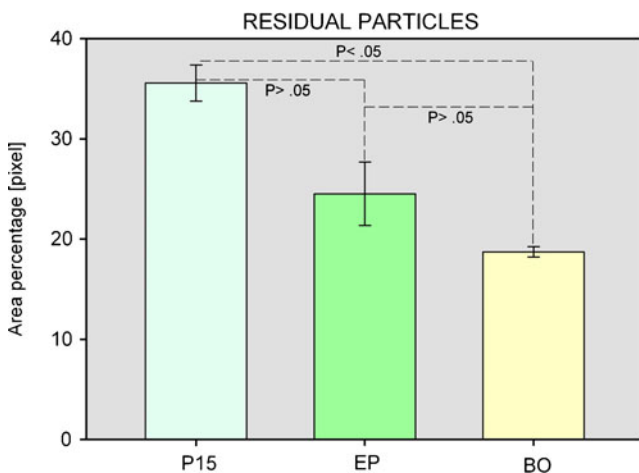


Fig. 2 Comparison of area percentage of residual particles among the biomaterials. Kruskal–Wallis and Tukey tests

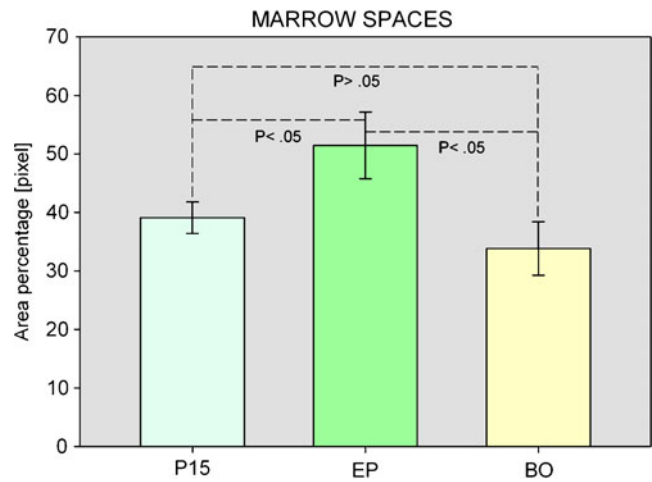


Fig. 3 Comparison of area percentage of marrow spaces among the biomaterials. Kruskal–Wallis and Tukey tests

fibers represented (mean rate \pm SD) $18.4\pm 2.7\%$, while the longitudinal collagen fibers represented (mean rate \pm SD) $16.3\pm 1.8\%$; the difference was not statistically significant ($P = .195$; Fig. 4, A1). The mineralized bone matrix in EP specimens appeared to be mainly formed by collagen fibers randomly oriented with a few areas of osteoid tissue (Fig. 4, B). Transverse collagen fibers represented (mean rate \pm SD) $4\pm 0.7\%$, while the longitudinal collagen fibers represented (mean rate \pm SD) $7.6\pm 2.5\%$. The difference was statistically significant ($P < .05$; Fig. 4, B1). The P-15 particles appeared surrounded by newly formed bone with collagen fibers randomly oriented, while in some areas, the collagen fibers were transversally oriented (Fig. 4, C). Transverse collagen fibers represented (mean rate \pm SD) $3.8\pm 1.6\%$, while the longitudinal collagen fibers represented (mean rate \pm SD) $4.9\pm 1.2\%$. The difference was not statistically significant ($P > .05$; Fig. 4, C1).

SEM-EDS

Under SEM, using backscattered electron signals, the biomaterial particles appeared in white-grey due to the high atomic number of the HA, while the newly formed bone appeared in dark-grey since it also contained some collagen, marrow, fat, and non-collagen proteins. The EDS analysis performed with spot analysis for elements showed a Ca/P ratio of 1.8 at/at.% for BO (Fig. 5a), a Ca/P ratio of 2.2 at/at.% for EP (Fig. 5b), while the Ca/P ratio was approximately 1.5 at/at.% for P-15 (Fig. 5c).

Discussion

Autogenous bone is thought to be the gold standard material for bone grafting techniques; nevertheless, it needs

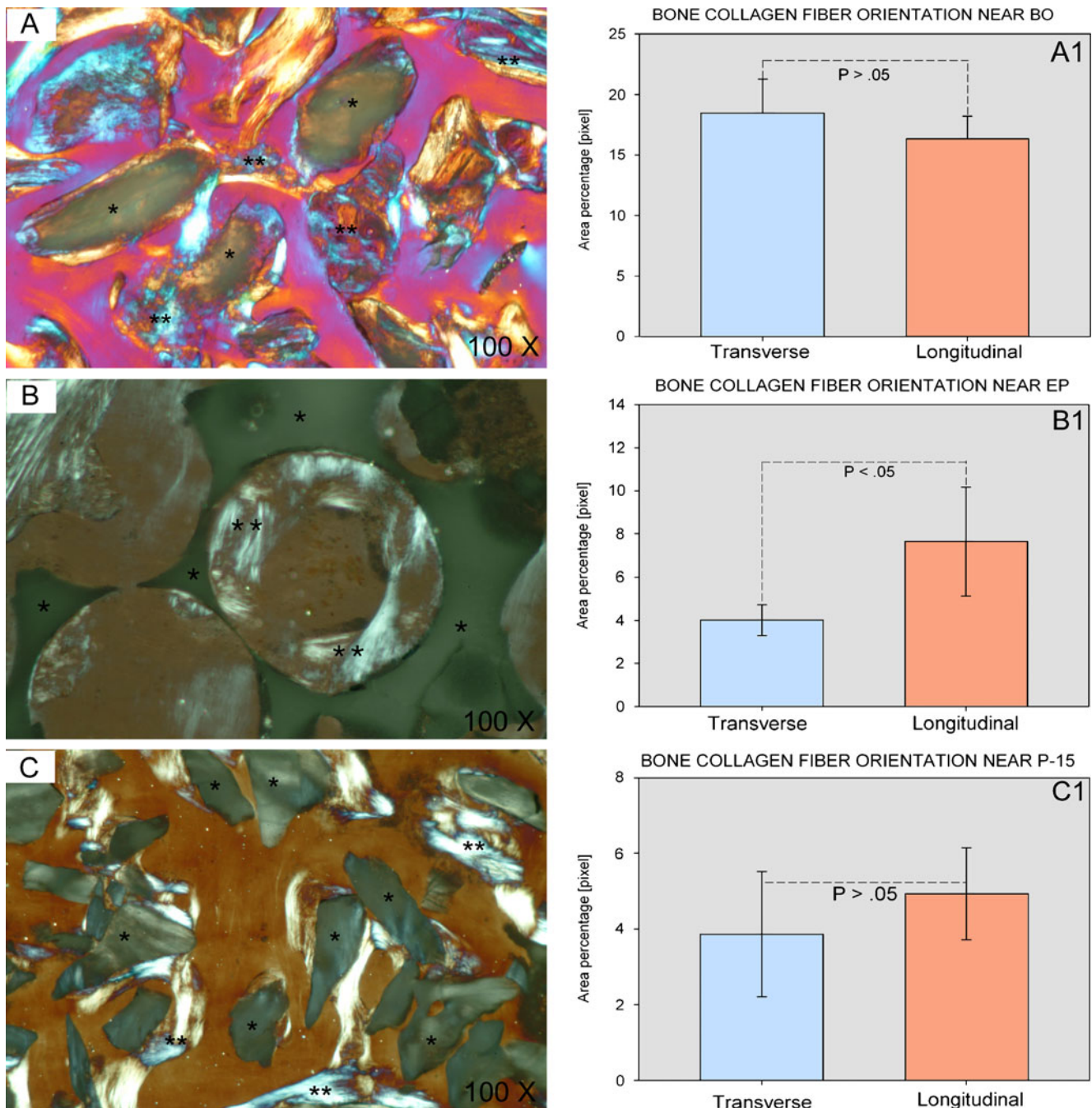


Fig. 4 *A* At $\times 100$ magnification, around the BO particles (double asterisks), bone transverse collagen fibers appeared in light blue, while bone longitudinal collagen fibers appeared in light yellow. *A1* Comparison for bone collagen fiber orientation. Unpaired *t* test. *B* At $\times 100$ magnification, around the EP particles (double asterisks), bone transverse collagen fibers appeared in light blue, while bone longitudinal

collagen fibers appeared in light yellow. *B1* Comparison for bone collagen fiber orientation. Unpaired *t* test. *c* At $\times 100$ magnification, around the P-15 particles (double asterisks), bone transverse collagen fibers appeared in light blue, while bone longitudinal collagen fibers appeared in light yellow. *C1* Comparison for bone collagen fiber orientation. Unpaired *t* test

additional surgery for donor sites and may imply additional complications to the patients as well as to the clinicians. Hence, many different bone substitutes emerged as an alternative to overcome these deficiencies. Many techniques and biomaterials have been tested, showing good results [45]. The bone augmentation has the teleological

purpose of bringing the affected tissue to a state of low entropy: regeneration, without permanent damage (*restitutio ad integrum*), and repair, with a tissue adaptation to functional tasks (*methaplasia*). The ideal scaffold of bone substitutes used in sites treated with implants should be characterized by a balance between mechanical stability

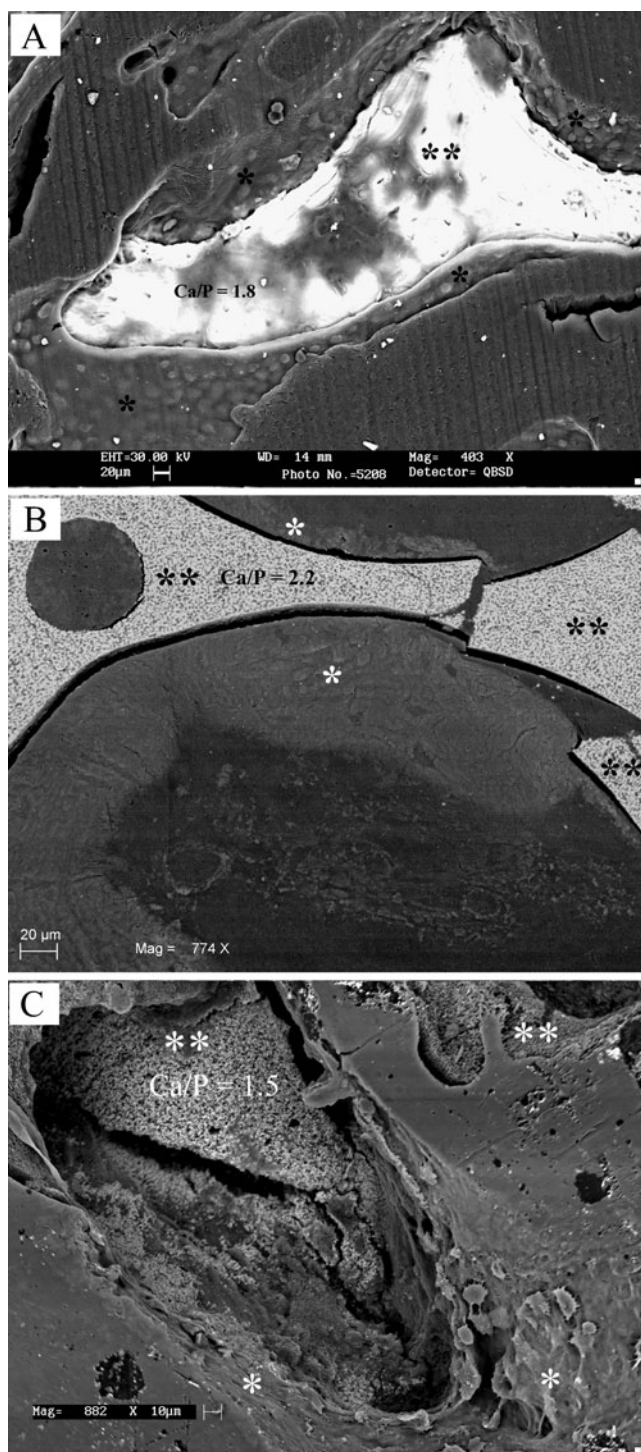


Fig. 5 **a** Backscattered electron image of BO particle (*double asterisks*) with surrounding newly formed bone (*single asterisks*). The Ca/P ratio of the particles was 1.8 ($n=10$). **b** Backscattered electron image of EP particle (*double asterisks*) with surrounding newly formed bone (*single asterisks*). The Ca/P ratio of the particles was 2.2 ($n=10$). **c** Backscattered electron image of P-15 particle (*double asterisks*) with surrounding newly formed bone (*single asterisks*). The Ca/P ratio of the particles was 1.5 ($n=10$)

and biodegradation. The substitution of the biomaterial should be completed in 6 months with direct substitution by newly formed bone without any transitional soft tissue. Moreover, after sinus lift augmentation in case of implant placement under immediate loading condition, the amount of load should be strictly related to the amount and quality (density) of crestal bone and, finally, the number and diameters of the inserted implants. As consequence, an important issue concerns the possibility of adapting the clinical use of the biomaterials in function of the specific patient needs. Yet, different growth patterns of the bone, in function of the scaffold composition/design of graft materials, presented different behaviors and responses. This preliminary human histological evaluation was done to improve the clinical use of the bone substitutes in implant dentistry. The results obtained from this study confirmed the advantageous use of BO in some cases. In fact, the newly formed network of bone with well-integrated particles remnants formed a continuous composite structure with a potentially functional capability [18]. The composite tissue bone plus biomaterial fulfilled the objectives of bone augmentation. Nevertheless, the mechanical competence of the biomaterials particles should be taken into the consideration especially in case of implant placement under loading condition. The BO particles retained approximately one third of their compressive strength [46]. Inadequate mechanical performance of grafts resulted in a mismatch in the mechanical properties of the augmented tissue relative to the native crestal bone, leading to tissue damage (resorption) or implant failure. In the present study, many residual particles of the biomaterial appeared enveloped and joined by means of newly formed bone without a significant resorption. The absence of resorption of the biomaterials, as we postulated [5], should be related to the relatively high calcium content. The evaluation of collagen fiber orientation in the new bone showed an absence of a predominantly spatial orientation, with no dominance between transverse and longitudinal fibers, showing a newly formed bone of woven type. BO showed significantly more bone > less residual particles > less marrow spaces; P-15 presented less bone > more residual particles > more marrow spaces; while for EP, the relation was inverted: more bone > less residual particles > more marrow spaces. An explanation for this fact could be related to the scaffold design of the biomaterial. Large pores were characterized by circumferential bone formation with a

central marrow space. The porous architecture of the HA substratum in EP, with its macro–micro pores network interconnections, could induce new bone formation. As reported by Ripamonti in several studies [21, 26, 28, 30], concavities are the ideal structural and biological micro-environment for the promotion of new bone formation because they induce rapid vascular and mesenchymal invasion and provide a specific pathway for cellular migration: these cells can attach, proliferate, and finally differentiate into functional osteoblasts. Moreover, the prevalence of the bone marrow spaces showed that the quality of newly formed bone was affected by the structure of the biomaterial: in the present study, inside the macroporosities of EP particles, bone tissue was arranged to fill the cavities, progressing from the inner surface of the pores to the center, in a symmetrical manner, with the collagen fibers arranged parallel to the long axis of osteoblasts. The histological and microstructural results about P-15 are similar to those of Barbosa et al. [35] who found bone formation in close association with the biomaterial particles and to those of Krauser et al. [41] who found that most of the biomaterial particles were connected and surrounded by newly formed bone. They are also consistent with previous results reported from our laboratory [47, 48]. This is, according to our knowledge, the first report on the bone response to P-15 under CPLM and SEM. The data support previous observations that the granules of P-15 become colonized with newly formed bone and that they are surrounded by osteoid. The SEM images showing the apparent penetration of non-mineralized tissue into the particles were particularly interesting. Clinical implications of the present observations appear to be irrelevant in cases of bone augmentation for esthetic/prosthetic reasons without implant placement. On the contrary, they are important for those cases in which the use of bone graft substitutes is an essential pretreatment for implant prosthetic restorations. The immediate load condition should be cautiously applied in case of less than 3 mm of crestal bone between sinus floor and alveolar ridge.

Conclusions

Within the limitation of the present study, the following conclusions could be drawn:

1. All the biomaterials used in this study demonstrated a close integration with the surrounding bone, confirming their biocompatibility and effectiveness for bone regeneration in maxillary sinus augmentation procedures.
2. No biomaterial was completely resorbed.
3. BO and P-15 showed the ability to form a “composite” network made of new bone with embedded biomaterial particles.

4. The microstructure of EP seems to favor the apposition of new bone inside the small pores.

Conflicts of interest The authors declare that they have no conflicts of interest.

References

1. Furst G, Gruber R, Tangl S et al (2003) Sinus grafting with autogenous platelet-rich plasma and bovine hydroxyapatite. A histomorphometric study in minipigs. *Clin Oral Implants Res* 14:500–508
2. Tatum OH (1986) Maxillary and sinus implant reconstruction. *Dent Clin North Am* 30:207–229
3. Tatum OH Jr, Lebowitz MS, Tatum CA, Borgner RA (1993) Sinus augmentation: rationale, development, long-term results. *NY State Dent J* 59:43–48
4. Orsini G, Traini T, Scarano A, Degidi M, Perrotti V, Piccirilli M, Piattelli A (2005) Maxillary sinus augmentation with Bio-Oss particles: a light, scanning, and transmission electron microscopy study in man. *J Biomed Mater Res B Appl Biomater* 74:448–457
5. Traini T, Degidi M, Sammons R, Stanley P, Piattelli A (2008) Histologic and elemental microanalytical study of anorganic bovine bone substitution following sinus floor augmentation in humans. *J Periodontol* 79:1232–1240
6. Piattelli M, Favero GF, Scarano A, Orsini G, Piattelli A (1999) A bone reactions to anorganic bovine bone (Bio-Oss) used in sinus lifting procedure: a histologic long-term report of 20 cases in man. *Int J Oral Maxillofac Implants* 14:835–840
7. Piattelli A, Scarano A, Quaranta M (1997) High-precision, cost-effective cutting system for producing thin sections of oral tissues containing dental implants. *Biomaterials* 18:577–579
8. Valentini P, Abensur D (1997) Maxillary sinus floor elevation for implant placement with demineralized freeze-dried bone and bovine bone (Bio-Oss®): a clinical study of 20 patients. *Int J Periodontics Restor Dent* 17:233–241
9. Wetzel AC, Stich H, Caffesse RG (1995) Bone apposition onto oral implants in the sinus area filled with different grafting materials. A histologic study in the beagle dogs. *Clin Oral Implant Res* 6:155–163
10. Tadjoeidin ES, de Lange GL, Bronckers ALJJ, Lyaruu DM, Burger EH (2003) Deproteinized cancellous bovine bone (Bio-OssR) as bone substitute for sinus floor elevation. A retrospective, histomorphometrical study of five cases. *J Clin Periodontol* 30:261–270
11. Froum SJ, Tarnow DP, Wallace SS, Rohrer MD, Cho SC (1998) Sinus floor elevation using anorganic bovine bone matrix (Osteograf/N) with and without autogenous bone: a clinical, histologic, radiographic, and histomorphometric analysis—part 2 of an ongoing prospective study. *Int J Periodontics Restor Dent* 18:529–543
12. Wheeler SL (1997) Sinus augmentation for dental implants: the use of alloplastic materials. *J Oral Maxillofac Surg* 55:1287–1293
13. Blomqvist JE, Alberius P, Isaksson S, Linde A, Obrant K (1998) Importance of bone graft quality for implant integration after maxillary sinus reconstruction. *Oral Surg Oral Med Oral Pathol Oral Radiol Endo* 86:268–274
14. Merx MAW, Maltha JC, Freihofer HP, Kuijpers-Jagtman AM (1999) Incorporation of particulated bone implants in the facial skeleton. *Biomaterials* 20:2029–2035

15. Ozaki W, Buchman SR (1999) Volume maintenance of onlay bone grafts in the craniofacial skeleton: micro-architecture versus embryologic origin. *Plast Reconstr Surg* 102:291–299
16. Wallace SS, Froum SJ, Tarnow DP (1996) Histologic evaluation of sinus elevation procedure: a clinical report. *Int J Periodont Restor Dent* 16:47–51
17. Wallace SS, Froum SJ (2003) Effect of maxillary sinus augmentation on the survival of endosseous dental implants. A systematic review. *Ann Periodontol* 8:328–343
18. Traini T, Valentini P, Iezzi G, Piattelli A (2007) A histologic and histomorphometric evaluation of anorganic bovine bone retrieved 9 years after a sinus augmentation procedure. *J Periodontol* 78:955–961
19. McDowell H, Gregory TM, Brown WE (1977) Solubility of Ca5 (PO4)3OH in the system Ca(OH)2-H3PO4-H2O at 5; 15; 25; and 378 C. *J Res Natl Bur Stand* 81A:273–281
20. Bigi A, Cojazzi G, Panzavolta S et al (1997) Chemical and structural characterization of the mineral phase from cortical and trabecular bone. *J Inorg Biochem* 68:45–51
21. Ripamonti U, Crooks J, Kirkbride AN (1999) Sintered porous hydroxyapatite with intrinsic osteoinductive activity: geometric induction of bone formation. *South Afr J Sci* 95:335–343
22. Yamasaki H, Saki H (1992) Osteogenic response to porous hydroxyapatite ceramics under the skin of dogs. *Biomaterials* 13:308–312
23. Yuan H, Li Y, Yang Z, Feng J, Zhang X (1997) An investigation on the osteoinduction of synthetic porous phase-pure hydroxyapatite ceramic. *Biomed Eng Appl Bas Com* 9:274–278
24. Healy KE, Harbers GM, Barber TA, Sumner DR (2000) Osteoblast interactions with engineered surfaces. In: Davies JE (ed) *Bone engineering*, vol 24. EM Squared Inc., Toronto, pp 268–281
25. Davies JE, Hosseini MM (2000) Histodynamics of endosseous wound healing. In: Davies JE (ed) *Bone engineering*, vol 1. EM Squared Inc., Toronto, pp 1–14
26. Ripamonti U (1996) Osteoinduction in porous hydroxyapatite implanted in heterotopic sites of different animal models. *Biomaterials* 17:31–35
27. Ripamonti U (1991) The morphogenesis of bone in replicas of porous hydroxyapatite obtained from conversion of calcium carbonate exoskeletons of coral. *J Bone Jt Surg* 73A:692–703
28. Ripamonti U (1990) Inductive bone matrix and porous hydroxyapatite composites in rodents and in non-human primates. In: Yamamuro T, Wilson-Hench J, Hench L (eds) *Handbook of bioactive ceramics*. CRC Press, Boca Raton, pp 245–253
29. Nanci A, Zalzal S, Fortin M, Mangano C, Goldberg HA (2000) Incorporation of circulating bone-matrix proteins by implanted hydroxyapatite and at bone surfaces: implications for cement-line formation and structuring of biomaterials. In: Davies JE (ed) *Bone engineering*. EM Squared Inc., Toronto, pp 305–311
30. Ripamonti U, Van den Heever B, van Wyk J (1993) Expression of the osteogenic phenotype in porous hydroxyapatite implanted extraskeletally in baboons. *Matrix* 13:491–502
31. Kuboki Y, Takita H, Kobayashi D et al (1998) BMP-induced osteogenesis on the surface of hydroxyapatite with geometrically feasible and nonfeasible structures: topology of osteogenesis. *J Biomed Mater Res* 39(2):190–199
32. Fiorellini JP, Weber HP (1994) Clinical trials on the prognosis of dental implants. *Periodontol* 4:98–108
33. van Eeden S, Ripamonti U (1994) Bone differentiation in porous hydroxyapatite is regulated by the geometry of the substratum: implications for reconstructive craniofacial surgery. *Plast Reconstr Surg* 93:959–966
34. Mangano C, Bartolucci E (2003) A new porous hydroxyapatite for promotion of bone regeneration in maxillary sinus augmentation: clinical and histological study in humans. *Int J Oral Maxillofac Implants* 18:20–30
35. Barbosa EP, de Souza RO, Caula AL, Neto LG, Caula FDE O, Duarte ME (2002) Bone regeneration of localized chronic alveolar defects utilizing cell binding peptide associated with anorganic bovine-derived bone mineral: a clinical and histological study. *J Periodontol* 73:1153–1159
36. Hanks T, Atkinson BL (2004) Comparison of cell viability on anorganic bone matrix with or without P-15 cell binding peptide. *Biomaterials* 25:4831–4836
37. Yukna RA, Krauser JT, Callan DP, Evans GH, Cruz R, Martin M (2002) Thirty-six follow-up of 25 patients treated with combination anorganic bovine-derived hydroxyapatite matrix (ABM) cell-binding peptide (P-15) bone replacement grafts in human infrabony defects. I. Clinical findings. *J Periodontol* 73:123–128
38. Thorwarth M, Schultze-Mosgau S, Wehran F et al (2005) Bioactivation of an anorganic bone matrix by P-15 peptide for the promotion of early bone formation. *Biomaterials* 26:5648–5657
39. Nguyen H, Qian JJ, Bhatnagar RS, Li S (2003) Enhanced cell attachment and osteoblastic activity by P-15 peptide-coated matrix in hydrogels. *Biochem Biophys Res Commun* 311:179–186
40. Hahn J, Rohrer MD, Tofe AJ (2003) Clinical, radiographic, histologic, and histomorphometric comparison of PepGen P-15 particulate and PepGen P-15 Flow in extraction sockets: a same-mouth case study. *Implant Dent* 12:170–174
41. Krauser JT, Rohrer MD, Wallace SS (2000) Human histologic and histomorphometric analysis comparing Osteograf/N with PepGen P-15 in the maxillary sinus elevation procedure: a case report. *Implant Dent* 9:298–302
42. Radhakrishnan S, Anusaya CN (2004) Comparative clinical evaluation of combination anorganic bovine-derived hydroxyapatite matrix (ABM)/cell binding peptide (P-15) and open flap debridement (DEBR) in human periodontal osseous defects: a 6 month pilot study. *J Int Acad Periodontol* 6:101–107
43. Thorwarth M, Schultze-Mosgau S, Wehrman F et al (2005) Enhanced bone regeneration with a synthetic cell-binding peptide—in vivo results. *Biochem Biophys Res Commun* 329:789–795
44. Trasatti C, Spears R, Gutmann JL, Opperman LA (2004) Increased TGF-beta1 production by rat osteoblasts in the presence of PepGen P-15 in vitro. *J Endod* 30:213–217
45. Esposito M, Grusovin MG, Coulthard P, Worthington HV (2006) The efficacy of various bone augmentation procedures for dental implants: a Cochrane systematic review of randomized controlled clinical trials. *Int J Oral Maxillofac Implants* 21:696–710
46. Spector M (1998) Basis principle of tissue engineering. In: Lynch SE, Genco RJ, Marx RE (eds) *Tissue engineering applications in maxillofacial surgery and periodontics*. Quintessence Publishing Co. Inc., Carol Stream, pp 3–16
47. Degidi M, Piattelli M, Scarano A, Iezzi G, Piattelli A (2004) Maxillary sinus augmentation using a synthetic cell-binding peptide. Histological and histomorphometrical results in man. *J Oral Implantol* 30(6):276–383
48. Scarano A, Iezzi G, Petrone G et al (2003) Cortical bone regeneration with a synthetic cell-binding peptide: a histologic and histomorphometric pilot study. *Implant Dent* 12(4):318

Copyright of Clinical Oral Investigations is the property of Springer Science & Business Media B.V. and its content may not be copied or emailed to multiple sites or posted to a listserv without the copyright holder's express written permission. However, users may print, download, or email articles for individual use.